Computational Materials Science 156 (2019) 321–324

Contents lists available at ScienceDirect

Computational Materials Science

journal homepage: www.elsevier.com/locate/commatsci

Strain effect of high Tc ferromagnetism in Mo-doped SnS_2 monolayer

Yaming Liu[a], Mingchao Liang[a], Bo Hu[a], Yongfeng Li[a], Jianxiu Su[a], Congxin Xia[b,*]

[a] Henan Institute of Science and Technology, Xinxiang 453003, China
[b] Henan Normal University, Xinxiang 453003, China

ARTICLE INFO

Keywords:
Ferromagnetism
Strain effect
DFT
Mo-doped SnS_2 monolayer

ABSTRACT

Endowing the nonmagnetic 2D materials with room temperature ferromagnetism (RTFM) is imperative for low-dimensional spintronic applications. Here, the electronic and magnetic properties of Mo-doped SnS_2 monolayer are investigated using first-principles calculations. Numerical results show that the Mo dopant induces a magnetic momentum of $2\mu_B$, which can be attributed to the 2 spin-parallel Mo *4_d* electrons that occupy the t_{2g} orbitals split by D_{3d} crystal field. Based on mean-field theory and Heisenberg model, Curie temperature (T_C) is calculated to be 865.7 K. Applying biaxial strain, the doped system shows half-metallic characteristics in the range −10% to +4%. Beyond +4%, a transformation from half-metal to semiconductor occurs. Due to the symmetry-reserved crystal structure, the compound exhibits robust magnetic momentum of $2\mu_B$ in the affordable biaxial strain range. Our calculations imply that Mo-doped SnS_2 monolayer is a high T_C strong ferromagnetism, and can be a promising candidate for new spintronic devices.

1. Introduction

Thanks to the intriguing physical and chemical properties, such as peculiar layered-structure, proper bandgap ~2.0 eV [1,2], high optical absorption coefficient > 10^4 cm^{-1} in visible range [3], non-toxic and excellent chemical stability in acid conditions [4], SnS_2 nanostructures are widely used for next-generation ultrathin and flexible optoelectronic devices, photocatalyst, photodetector, lithium-ion battery, field effect transistors and photovoltaic cell [5–12], etc. Unfortunately, the nonmagnetic property of perfect SnS_2 monolayer nanosheet hampers the applications in spintronic field [13]. Endowing SnS_2 nanostructures with room temperature ferromagnetism (RTFM) receives tremendous attentions in recent years. Among the universal methods, for example dimensionality-reduction (nanoribbon), defect-induction and applying strain, doping metal atoms into two-dimensional (2D) nanostructures is a straightforward way for introducing the magnetic characteristics. Up to now, many theoretical and experimental studies reported the induced magnetic momentum of doped SnS_2 nanosystems. Mainly focused on the optical properties, Sun *et al.* theoretically studied the Fe-, Zn-doped SnS_2 systems. The absorption efficiencies are enhanced and both of the impurity atoms can induce magnetic moments about $2\mu_B$ per dopant [14–16]. Gao *et al.* find that RTFM property can be tuned by the porosity in porous SnS_2 nanosheets [17]. Prabha D. *et al.* synthesized the Al- and Sr-doped SnS_2 nanopowders with different concentrations, and the induced magnetic and antifungal properties are discussed [18,19]. Doping Zr into SnS_2 nanostructure, the doped samples exhibit both ferromagnetic ordering and the improved antibacterial efficiency [20]. Xiao *et al.* systematically discussed the *4d* transition metal doped SnS_2 monolayer [21]. Different with Srivind's experiments [20], they found that both Zr- and Pd-doped systems remain nonmagnetic semiconductors. However, Nb- and Mo-doped complex displays long-ranged ferromagnetism ordering with Curie temperature high above room temperature. In our previous works, the effects of strain on Fe-doped SnS_2 are systematically discussed [22]. The induced magnetic momentum is about $1.986\mu_B$ per Fe atom and the biaxial strain leads to a transformation from half-metal to metal/semiconductor under tensile/compressive strain. Despite these amounts of descriptions about electronic and geometrical structures of doped SnS_2 nanostructures, both theoretically and experimentally, the magnetic properties and the responsible mechanism for the fundamental magnetism are still not fully understood. In this work, the structural, electronic, magnetic properties and effect of biaxial strains are systematically discussed. Though the most stable configurations of monolayer SnS_2 and MoS_2 are all nonmagnetic semiconductors, the Mo doped SnS_2 nanosheets, due to the crystal field splitting, exhibit strong ferromagnetism with a Curie temperature (T_C) as high as 865.7 K, and the induced ferromagnetic characteristics are robust under the affordable biaxial strain conditions from −10% to +10%. The present work provides a route to harness the magnetic properties of 2D SnS_2 for spintronic applications.

* Corresponding author.
E-mail address: xiacongxin@htu.cn (C. Xia).

https://doi.org/10.1016/j.commatsci.2018.10.010
Received 8 August 2018; Accepted 9 October 2018

2. Computational methods

All the calculations in this work are carried out within the framework of spin-polarized density functional theory as implemented in VASP [23,24]. Projector-augmented wave and Perdew–Burke–Ernzerhof generalized gradient approximation (PBE-GGA) are adopted for describing the core-electron interactions and exchange-correlation potential, respectively [25–27]. The plane-wave kinetic energy cutoff is set to be 520 eV. The Monkhorst-Pack scheme of k-point sampling is used for integration over the first Brillouin zone [28]. A $5 \times 5 \times 1$ and $11 \times 11 \times 1$ Γ–centered k-mesh sampling is used for relaxation and static calculation, respectively. The convergence threshold is 10^{-5} eV for energy and 10^{-3} eV/Å for forces. A vacuum space of 15 Å is adopted to model the $4 \times 4 \times 1$ supercell for avoiding the interactions between periodical slabs. On-site Hubbard U parameters (= 9.0 eV) is performed to treat the effect of on-site repulsion of Sn_*4d* states, which has been verified successfully in several present works [29]. While several U (= 2, 3, 4, 5 eV) are tested for Mo_*4d* orbitals, which yields almost the same results [30,31].

3. Results and discussion

3.1. Structure and electronic properties of SnS_2 monolayer

We firstly examined the geometrical structure and electronic properties of perfect SnS_2 monolayer. As a typical compound of layered metal dichalcogenides, the Sn atomic layers coordinate with two S atomic layers to form an S-Sn-S sandwiched monolayer structure. Periodically stacking along *c*-axis, these monolayers are weakly coupled via van der Waals interactions, and can be easily exfoliated through mechanical and scalable liquid exfoliation strategy [7,32].

SnS_2 monolayer crystallizes in hexagonal symmetry with space group P-3m1 (No. 164), and the Sn and S atoms lie in 1b (0, 0, 0.5) and 2d (1/3, 2/3, *z*), (2/3, 1/3, -*z*) Wyckoff sites, where *z* is variable inner parameter. In this work, the optimized *z* is 0.5826. A $4 \times 4 \times 1$ supercell of pristine SnS_2 monolayer presents in Fig. 1, and the optimized lattice constants are listed in Table 1. The calculated parameters agree well with previous theoretical and experimental reports.

Based on the optimized parameters, the electronic properties of pristine SnS_2 monolayer are calculated and analyzed in Fig. 1(b). From the band structure, we find the valence band maximum and conduction band minimum locate near Γ and M, respectively, indicating the indirect semiconducting characteristics with bandgap of 2.362 eV. Checking spin-polarized total and partial density of states, we find that the valence band maximum is composed of S_*3p* states, while the conduction band minimum is dominated by Sn_*5p* and S_*3p* orbitals. The hybridization of Sn_*5p* and S_*3p* orbitals indicate a covalent bond character, which is typical for layered metal dichalcogenides, and has been certified in previous works [14]. Rechecking Fig. 1(b), the other remarkable feature is the symmetric spin-up and spin-down lines, which indicate the nonmagnetic ground state.

Table 1
Lattice constants *a*, S-Sn bond lengths $d_{S\text{-}Sn}$ and band gaps E_g of SnS_2 monolayer calculated with different DFT frameworks, and compared with previous theoretical and experimental reports.

	a (Å)	$d_{S\text{-}Sn}$ (Å)	E_g (eV)
PBE	3.689	2.591	1.650
PBE + *U*	3.482	2.437	2.362
Exp. [7]	3.700	2.600	2.230
Theo. [33]	3.522	2.468	2.224

3.2. Electronic and magnetic properties of Mo-doped SnS_2 monolayer

Being highly crystalline and defect-free, and able to sustain remarkably large elastic strain, both monolayer SnS_2 and MoS2 are ideal candidates for gapless graphene, and received tremendous attentions in recent years. Disappointingly, both of them show no spin polarization in monolayer configurations. To modify the magnetic properties, we dope one Mo atom into a 4×4 SnS_2 monolayer to modulate the magnetism. The doped Mo atom is marked *0* in Fig. 1(a), and the formation energies E_{form} is calculated under Sn- and S-rich conditions to verify the structural stability [34].

$$E_{form} = E_{doped} - - E_{pristine} + \mu_{Sn} - - \mu_{Mo}$$

in which E_{doped} and $E_{pristine}$ are the calculated total energies of monolayer SnS_2 with and without Mo dopant. Chemical potential μ_X depends on the growth conditions, and the most energetically stable phase for Mo (*Im-3m*, No.229), Sn (*Fd-3m*, No.227) and S2 molecular are adopted. Thus, the formation energies of Mo-doped systems are 2.094 eV and −2.356 eV for Sn-rich and S-rich growth conditions, respectively. The lower negative E_{form} in S-rich condition indicates that it is easier to incorporate Mo into SnS_2 nanosheet and form energetically stable complex.

In order to determine the magnetic ground state, the energy difference between nonmagnetic and magnetic states, *i.e.* $E_{nonmag} - E_{mag}$, is calculated to be 0.477 eV, indicate that the magnetic ground state with $2\mu_B$ per Mo atom is more stable. To further illustrate the nature of the Mo-induced magnetism, Fig. 2 shows the spin-polarized electronic DOS and spin charge density distribution. The spin-charge density ($\rho_{up} - \rho_{down}$) clearly shows that the spin-polarized charges are concentrated to the dopant Mo atom, and coincide with the calculated magnetic moment of $2\mu_B$/unit cell.

Viewing Fig. 2(b) and comparing with Fig. 1, we find that the significant distinction is the half-metallic and magnetic characteristics of Mo-doped system. In the framework of crystal field theory, the magnetism nature can be attributed to the symmetry-induced splitting. Due to the D_{3d} symmetry, the Mo_*4d* orbitals of an O_h-MoS_6 unit split into two groups: low-energy triple-degenerated t_{2g} (d_{xy}, d_{yz}, d_{xz}) and high-

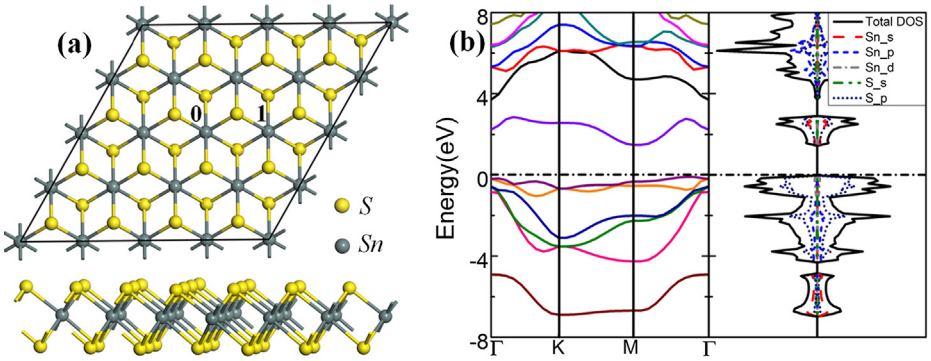

Fig. 1. Geometrical structure, electronic (atom-resolved) DOS and band structure of 4×4 SnS_2 monolayer. Sn atoms marked 0 and 1 indicates the dopant sites.